Behavior of Crystalline Xe Nanoprecipitates during Coalescence

R. C. Birtcher,[1] S. E. Donnelly,[2] M. Song,[3] K. Furuya,[3] K. Mitsuishi,[3] and C. W. Allen[1]
[1]*Materials Science Division, Argonne National Laboratory, Argonne, Illinois 60439*
[2]*Joule Physics Laboratory, University of Salford, Manchester M5 4WT, United Kingdom*
[3]*National Research Institute for Metals, 3-13 Sakura, Tsukuba 305, Japan*
(Received 18 December 1998)

In situ high-resolution electron microscopy has been used to observe nanoprecipitates of crystalline Xe in faceted cavities in Al during coalescence induced by 1.0 MeV electron irradiation at 300 K. Atomic-level fluctuations of cavity facets result in shape changes and precipitate motion leading to coalescence. There is no apparent elastic interaction between precipitates separated by as little as 0.5 nm. After coalescence, crystalline Xe conforms by plastic deformation without melting to changes in cavity shape. Cavity volume, not surface area, is conserved during coalescence, implying that cavity pressure is not determined solely by the interface tension.

PACS numbers: 61.82.Bg, 61.46.+w, 61.80.Fe, 61.82.Rx

Noble-gas atoms are insoluble in metals and condense during implantation into nanometer-sized precipitates. Research on solid noble-gas precipitates in metals [1] (often referred to as bubbles) has established many aspects of their behavior, but has left unanswered questions regarding atomic level phenomena. In many cases, at small sizes the precipitates are crystalline and yield sharp electron diffraction patterns [2]. However, the detailed structure of nanometer-sized precipitates has not been adequately resolved or explained, nor have growth and migration mechanisms been established.

Models of precipitate structure, based on conventional transmission electron microscopy observations, have assumed ideal forms for internal and interface structures. Electron diffraction has shown that precipitates of heavier noble-gas atoms in fcc solids are solid fcc crystals mesotactic with the host; i.e., the precipitate and the host matrix exhibit the same crystal orientation, even though lattice parameters of the crystalline noble gases are significantly larger than those of their metallic host. For example, the lattice parameter of crystalline Xe is about 50% larger than that of Al, but the Xe lattice is still mesotactic with the Al lattice [3]. Although typically containing only a few hundred to a few thousand atoms, noble-gas atom precipitates appear to obey their bulk equilibrium phase diagram and to be under high pressures proportional to the surface tension of the host and the reciprocal of the radius of the cavity that they occupy [2–5]. Melting may result from local heating or from an increase in precipitate size that decreases the internal pressure below that required to maintain the crystalline state.

Solid Xe is highly compressible relative to Al, and the Xe density is controlled by the size of the cavity in the Al. If, as for the case of He bubbles, cavity pressure were controlled by surface tension γ and described by $2\gamma/r$ [6], where r is the cavity radius, surface area would be conserved after coalescence. This is observed during thermal or irradiation driven coalescence of He bubbles [7]. The implication is that He in bubbles acts like an ideal gas and that these bubbles are at equilibrium pressures determined by their sizes. At the other extreme of compressibility, coalescence of two incompressible precipitates, such as Co in Cu, would occur at constant total volume, and the total projected area would decrease by 20% if the final precipitate were able to become equiaxed. It has not been clear what to expect in the case of the coalescence of small, crystalline, but fairly compressible, precipitates of Xe.

Recent advances in high-voltage, high-resolution electron microscopy allow direct determination of the internal structures of nanometer-size precipitates. We have used an off-zone axis high-resolution transmission electron microscopy (HRTEM) technique [8,9] to observe the structure of Xe nanocrystals embedded in Al during electron irradiation. This technique has been used to follow the motion of a 1 nm crystalline Xe precipitate and the coalescence of two noncrystalline Xe precipitates during 1 MeV electron irradiation at room temperature [10]. Under these conditions, none of the small crystalline Xe precipitates was perfectly faceted, and the facet imperfections were unstable during observation. Surface diffusion of Al on the cavities containing fluid Xe was found to be responsible both for precipitate motion and for shape changes after coalescence. The current work examines the behavior of solid Xe during the coalescence of two 5 nm crystalline Xe precipitates under electron irradiation at room temperature and, in particular, the response of the crystalline Xe to the change in the cavity shape after coalescence and the physics of the coalescence process.

TEM specimens were prepared by electrochemical jet thinning of well-annealed, high purity Al disks to perforation. Thinned specimens were implanted at room temperature with 30 keV Xe ions to a total dose of 2×10^{19} m^{-2} at Argonne National Laboratory. This implantation produces a high density of crystalline Xe precipitates 2 to 5 nm in diameter. Specimens were sealed in a quartz tube filled with 1 atm of Ar and transported to Japan.

Observations and electron irradiations were performed with 1 MeV electrons at room temperature in the high-resolution high-voltage electron microscope (JEM-ARM 1000, JEOL Ltd.) [11] located at the National Research Institute for Metals in Tsukuba, Japan. The electron beam was incident near normal on a region of specimen having a ⟨011⟩ surface normal. The electron flux was relatively large, 6.6×10^{24} m^2 s^{-1}, yielding a damage rate in Al of approximately 3.9×10^{-2} displacements per atom (dpa) per second [12]. At room temperature, both Al interstitials and vacancies are mobile [12]. In the absence of sinks such as Xe precipitates, point defects would be expected to cluster into loops or to migrate to surfaces and to grain boundaries. The energy required for displacement of Al is 19 eV [13]; that of Xe is not known; however, it is expected that both Al and Xe atoms will be directly displaced by 1 MeV electrons. Under 1 MeV electron irradiation, recoiling Al atoms have a maximum recoil energy of 160 eV and could transfer as much as 90 eV to a Xe atom, which is significantly greater than the maximum of 33 eV that could be transferred directly by the electrons. Although Xe recoils may travel one or two Al lattice spacings, this is expected to result in a rather unstable Xe/Al interface structure and to be quickly recovered.

The specimen was imaged during the electron irradiation, and images were recorded on videotape at 30 frames per sec. To improve image quality, a running five frame average was performed. Details of the high-resolution off-axial imaging technique have been described previously [8,9]. The technique involves a few degrees of specimen tilt away from a 110 zone axis and appropriate non-Scherzer defocus to reduce the image contrast due to low order Al reflections. The result is a high-resolution image that has little contrast from the Al matrix while Xe atom columns containing as few as two atoms are imaged in good contrast [10]. Crystalline Xe precipitates are seen in ⟨011⟩ projection. In this orientation, one {200} and two {111} planes are projected edge-on. Multislice image simulations indicate that the dark spots in the lattice image under the conditions of defocus used in the experiment are projections of Xe atom columns [9].

When smaller than approximately 8 nm in diameter, Xe precipitates in Al are crystalline during TEM observation at 300 K [3]. However, the precipitate structure is not stable under 1 MeV electron irradiation. The motion and resultant coalescence of two crystalline Xe precipitates, well isolated from other precipitates, is shown in Fig. 1 by a sequence of nine video frames, extending over a time period of 727 sec, during continuous 1 MeV electron irradiation. In order to reveal details, the figure covers two extended periods before and after coalescence, and a short period during coalescence. Unobstructed observation of such events was rare.

Precipitate motion is clearly visible in Figs. 1(a)–1(c) that were extracted from the video recording during a 418 sec time period. At the start, the two precipitates appear in projection to be nearly equiaxed. The image of the solid Xe reveals the shape of the cavity in the Al that would otherwise not be clearly visible. Not all precipitate facets are perfectly flat, and their microstructure does not remain static. This is the case for all crystalline Xe precipitates observed. Steps on precipitate facets result in accommodation faulting of the crystalline Xe. Changes and motion of facet irregularities also produce precipitate motion.

During the first period of 418 sec, the precipitates approach within 2 Al lattice spacings of each other. The precipitates maintain a horizontal separation of 2 to 3 Al {111} planes without rapid connection. Although we cannot determine the vertical separation from a plan view, the image contrast and precipitate motion indicate that there was little vertical separation between the two precipitates. There is a lack of attractive interaction between the precipitates even near the vertices of the precipitates.

Before coalescence, the Xe lattice planes in the right precipitate are significantly distorted, and the column spacing in the image is different in the two ⟨111⟩ directions and varies along many rows of columns. The Xe lattice appears to be distorted by at least one planar defect, likely a stacking fault lying in an inclined {111} plane near the bottom right of this precipitate. Imperfections in the crystalline Xe are a response of the easily sheared noble-gas crystal to defects on the Al cavity surface. Comparison of the motion of crystalline and fluid precipitates indicates no significant difference in their migration rates. This is not surprising in view of the low shear and bulk moduli of crystalline Xe relative to those of Al.

Details of the coalescence process are shown in Figs. 1(d)–1(f); these images show a sequence of three video frames from a 2.1 sec period. During this time period, a fluctuation on the left {111} facet of the right precipitate results in contact between the precipitates. Penetration of the 2-atomic-layer-thick Al membrane between the crystalline Xe precipitates occurred at the site of one Xe column during the time required to record one (time-averaged) video frame or approximately $1/6$ second. The opening between the two Xe particles quickly enlarges as surface diffusion transfers Al away from the region.

Continued evolution of the new precipitate after coalescence is shown in Figs. 1(g)–1(i) by a sequence of three video frames extracted from a 168.8 sec long period after coalescence. Immediately following coalescence the precipitate shape is very far from equiaxed. The ratio of {200} to {111} surface areas greatly exceeds that found for the two individual Xe precipitates. During continued irradiation and observation, the precipitate approaches the more equiaxed equilibrium shape observed for the two original precipitates. This is achieved by movement of ledges on the irregular precipitate facets. During this period, the bulk Al received an irradiation dose of 6.5 dpa. It is expected that these displacements provide sufficient surface diffusion to reorder the facets on the cavity in the Al [10]. An

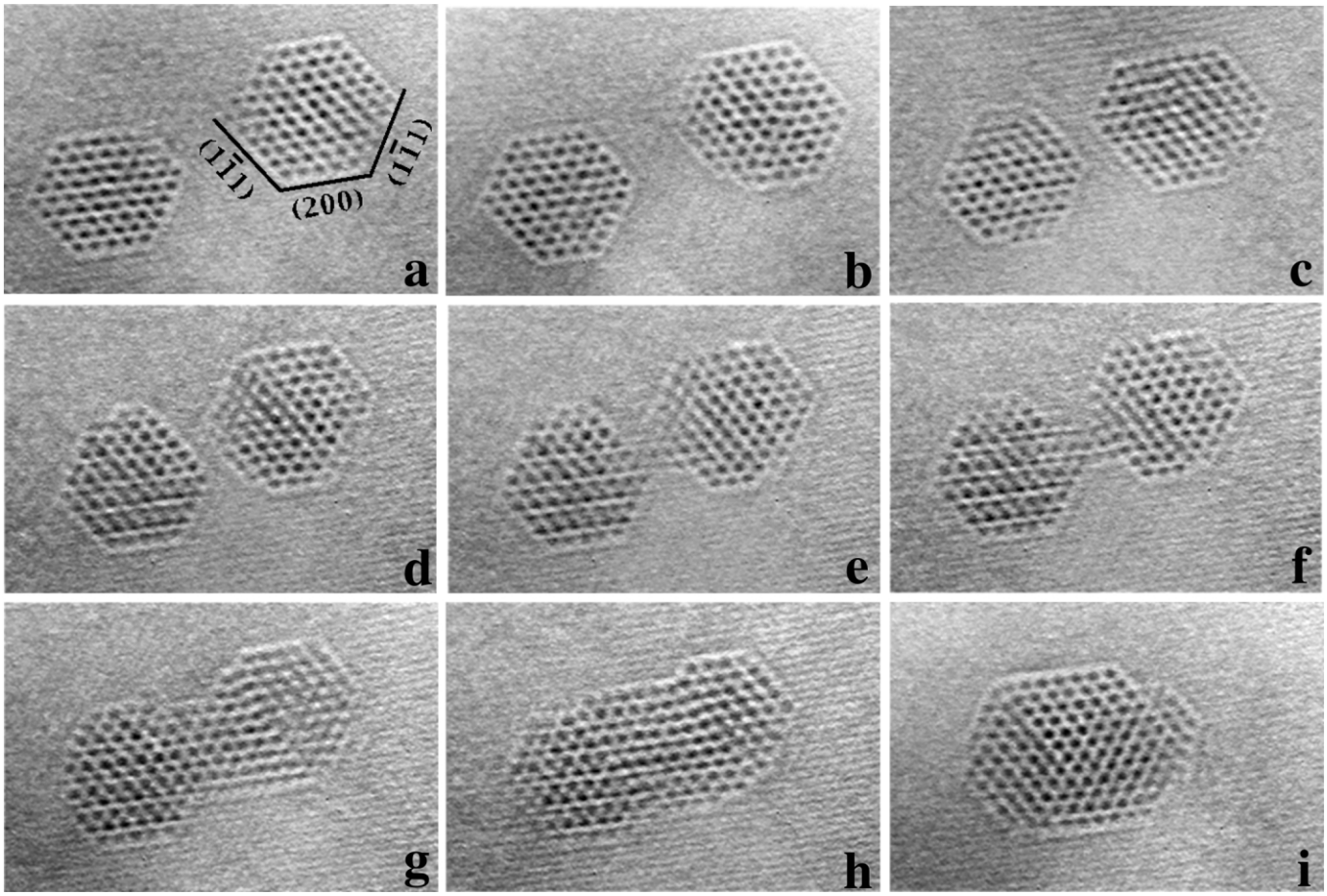

FIG. 1. Motion and coalescence of two isolated crystalline Xe precipitates during continuous 1 MeV electron irradiation. Measured from the first image, the elapsed times at which video frames were recorded are (a) 0, (b) 101, (c) 418, (d) 549, (e) 550, (f) 551, (g) 561, (h) 584, and (i) 727 seconds. Traces of crystallographic planes are indicated in frame (a).

unknown amount of damage was produced in the Xe by the electrons and by Al recoils.

The dynamic response of the crystalline Xe is striking. The crystalline Xe deforms by shear corresponding to the glide of dislocations (slip) in response to the reshaping of the irregular matrix cavity. Within our time resolution, the Xe atom columns made discrete jumps, and the changing shape of the Al cavity controlled their motion. The crystalline Xe conforms by slip to shape changes of its host cavity. In this sense, the crystalline Xe behaves somewhat like a fluid, however, at no time did the crystalline Xe precipitate melt.

After coalescence, complete transformation of the precipitate to an equiaxed shape required more than the 180 sec during which the precipitate could be observed. Immediately after the frame shown in Fig. 1(i), electron sputtering had removed sufficient Al that the Xe precipitate ruptured through the surface and disappeared. Rearrangement to form a more equiaxed precipitate shape after coalescence involves minimizing the total energy by balancing of relative areas of {111} and {200} facets and minimizing the number and length of steps on facets. This activity, due to Al surface diffusion at room temperature, is greatly enhanced by defects produced by electron irradiation. The shape change was driven primarily by motion of steps on Al {111} facets. This resulted in growth of the {111} facets and a concomitant reduction of the area of {200} facets. The ratio of the separation between the {111} and {200} facets approached 1.08, the value expected for an ideal cavity in Al, based on the Wulff construction [14]. Values of 1.04 to 1.10 are found for the original precipitates. The range of these values corresponds to differences produced by the addition of a single plane of Al atoms to such small cavities.

The effect of coalescence on the Xe lattice spacings can be determined from Fig. 1 through comparison with faintly visible Al (111) spacings. Before coalescence the Xe lattice parameter was 0.64 ± 0.01 nm in the left precipitate in Fig. 1 and between 0.65 and 0.67 nm in the right precipitate which is strongly distorted by defects. After coalescence the lattice parameter is 0.64 nm, implying little or no change in the Xe density. In addition, the number of projected Xe atom columns decreased to 130 in the final image of the coalesced precipitate, Fig. 1(i), from a total of 141 in the two initial precipitates, a decrease of 8%. Measurements of projected areas before and

after coalescence also yield a reduction of 8% so that the areal density of projected Xe atom columns remained unchanged. Both measurements indicate little or no change in Xe density.

The estimated decrease in the projected surface area of 8% is less than the 20% expected for volume conservation, but precipitate evolution had clearly not reached its conclusion of an equiaxed shape before the precipitate disappeared through the specimen surface. If further observations had been possible, we estimate that if the 17 Xe columns in weak contrast on the edges of the final observed precipitate were absorbed into an equilibrium shape, the projected area would decrease by the 20% required for volume conservation.

The Xe lattice parameters indicate little or no change of Xe density after coalescence, consistent with no change in total volume. The unchanged Xe lattice parameter also indicates that the pressure did not change. If the equilibrium pressure in a cavity is given by $P = 2\gamma/r$, both surface area and cavity pressure would decrease by 20% after coalescence of two identical precipitates if total volume were conserved. The Xe lattice parameter indicates that the pressure is unchanged and that the final precipitate should be overpressurized generating strain in the surrounding matrix. Image contrast from such strain has not been detected. It appears, unlike for He bubbles, that cavity pressure is affected by the interaction between the solid Xe and Al and not described solely by the surface tension.

Although the three dimensional shape of the cavity containing the Xe precipitates cannot be extracted from an image taken in only one crystallographic projection, precipitate shape and volume can be estimated by assuming that {200} facets are square. With this assumption, before coalescence, the two precipitates had volumes of approximately 13.2 nm^3 and 18.3 nm^3. After coalescence, the single precipitate in Fig. 1(i) is estimated to have a volume of 32.8 nm^3. The initial and final volumes differ by 4%. In spite of the uncertainty in these estimations, they suggest that the total volume, not the surface area, was conserved during the coalescence.

In summary, several points can be made about these observations. First, total precipitate volume, not surface area, appears to be conserved during coalescence of crystalline Xe precipitates implying that surface tension of the host material alone does not control the system. Second, to the level of two Al spacings in the $\langle 111 \rangle$ direction, there is no apparent attractive or repulsive elastic interaction between crystalline Xe precipitates. This is the strongest indication to date that crystalline Xe precipitates in Al do not generate strain in the Al lattice. This has also been reported for noncrystalline He bubbles in Al during heavy-ion irradiation [7]. Third, shape changes, random motion, and coalescence of crystalline Xe precipitates are caused by motion of steps on cavity facets as a result of irradiation. At any time, this roughness involves at most a few Al plane spacings. Fourth, shape changes of the cavity in the Al cause the crystalline Xe to deform plastically. At all times the Xe remains crystalline.

The authors are indebted to Bernard Kestel and Loren Funk at Argonne National Laboratory for specimen preparation and ion implantation. This work was performed under the Japan-USA Scientific Exchange Agreement and was supported at the respective laboratories by the U.S. Department of Energy (Contract No. W-31-109-Eng-38) and by the Science and Technology Agency of Japan. One of us (S. E. D.) acknowledges funding from both Argonne National Laboratory and the National Research Institute for Metals. Two of us (S. E. D., R. C. B.) acknowledge the support of NATO in the form of a collaborative research Grant No. 910670.

[1] *Fundamental Aspects of Inert Gases in Solids*, edited by S. E. Donnelly and J. H. Evans, NATO ASI, Ser. B, Vol. 279 (Plenum Press, New York, 1991).
[2] A. vom Felde, J. Fink, Th. Müller-Heinzerling, J. Pflüger, B. Scheerer, and G. Linker, Phys. Rev. Lett. **53**, 922 (1984).
[3] S. E. Donnelly and C J Rossouw, Science **230**, 1272 (1985).
[4] S. E. Donnelly, Radiat. Eff. **90**, 1 (1985).
[5] R. C. Birtcher and W. Jäger, J. Nucl. Mater. **135**, 274 (1985); R. C. Birtcher and W. Jäger, Ultramicroscopy **22**, 267 (1987).
[6] S. E. Donnelly, J. C. Rife, J. M. Gilles, and A. A. Lucas, J. Nucl. Mater. **93 & 94**, 767 (1980).
[7] R. C. Birtcher, S. E. Donnelly, and C. Templier, Phys. Rev. B **50**, 764 (1994).
[8] K. Tanaka, K. Kimoto, and K. Mihama, Ultramicroscopy **39**, 395 (1991).
[9] K. Furuya, N. Ishikawa, and C. W. Allen, J. Microsc. **194**, 152 (1999).
[10] C. W. Allen, R. C. Birtcher, S. E. Donnelly, K. Furuya, N. Ishikawa, and M. Song, Appl. Phys. Lett. **74**, 2611 (1999).
[11] K. Furuya, M. Piao, N. Ishikawa, and T. Saito, Mater. Res. Soc. Symp. Proc. **439**, 331 (1997).
[12] P. G. Lucasson and R. M. Walker, Phys. Rev. **127**, 485 (1962).
[13] H. M. Simpson and R. L. Chaplin, Phys. Rev. **185**, 958 (1969).
[14] W. W. Mullins, *Metal Surfaces*, edited by W. D. Robertson and N. A. Gjostein (American Society of Metals, New York, 1963), Chap. 2.